Estimation of the convergence order of rigorous coupled-wave analysis for binary gratings in optical critical dimension metrology

Shiyuan Liu
Huazhong University of Science and Technology
Wuhan National Laboratory for Optoelectronics
Wuhan 430074, China
and
Huazhong University of Science and Technology
State Key Laboratory of Digital Manufacturing Equipment and Technology
Wuhan 430074, China
E-mail: shyliu@mail.hust.edu.cn

Yuan Ma
Xiuguo Chen
Huazhong University of Science and Technology
Wuhan National Laboratory for Optoelectronics
Wuhan 430074, China

Chuanwei Zhang
Huazhong University of Science and Technology
State Key Laboratory of Digital Manufacturing Equipment and Technology
Wuhan 430074, China

Abstract. In most cases of optical critical dimension metrology, when applying rigorous coupled-wave analysis to optical modeling, a high order of Fourier harmonics is usually set up to guarantee the convergence of the final results. However, the total number of floating point operations grows dramatically as the truncation order increases. Therefore, it is critical to choose an appropriate order to obtain high computational efficiency without losing much accuracy in the meantime. We show that the convergence order associated with the structural and optical parameters is estimated through simulation. The results indicate that the convergence order is linear with the period of the sample when fixing the other parameters, both for planar diffraction and conical diffraction. The illuminated wavelength also affects the convergence of a final result. With further investigations concentrated on the ratio of illuminated wavelength to period, it is discovered that the convergence order decreases with the growth of the ratio, and when the ratio is fixed, convergence order jumps slightly, especially in a specific range of wavelength. This characteristic could be applied to estimate the optimum convergence order of given samples to obtain high computational efficiency. [DOI: 10.1117/1.OE.51.8.081504]

Subject terms: optical critical dimension metrology; rigorous coupled-wave analysis; convergence order; Fourier harmonics; binary gratings; optical modeling.

Paper 111067SSP received Sep. 1, 2011; revised manuscript received Oct. 7, 2011; accepted for publication Oct. 13, 2011; published online May 16, 2012.

1 Introduction

Nowadays, the critical dimension (CD) in integrated circuits is shrinking to 45 nm and even lower, accompanying with tremendous challenges of nanometrology.[1] The optical critical dimension (OCD) metrology, also called scatterometry,[2–4] is one of the well-known optical techniques that has gained considerable interest in the industrial environment because it is fast, noncontact, nondestructive, and of low-cost, compared to other techniques such as scanning electron microscopy (SEM) and atomic force microscopy (AFM).[5,6] The success of OCD metrology relies heavily on accurate forward modeling of sub-wavelength structures and fast extraction of structural parameters.[3] Starting from Maxwell's equations, either in integrated or differential form, the electric and magnetic fields can be obtained in the forward modeling problem, from which the reflectivity or ellipsometric parameters can be further calculated.[7–10] Then in the inverse problem, the measured optical parameters are obtained and utilized to fit the simulation parameters using some library search methods or nonlinear regression algorithms.[2,11,12] The forward modeling is repeated until the required accuracy is acquired and the structural parameters are measured to provide the best fit. Because this process takes time, it is highly desirable to improve the speed of optical modeling to achieve the greatest efficiency in OCD metrology.

Currently, the rigorous coupled-wave analysis (RCWA) method has been widely used in OCD metrology for the optical modeling of periodic structures.[8,13,14] When implementing this technique, the permittivity of the grating region is first expanded into a series of Fourier harmonics, then the electromagnetic field is expressed as a Fourier expansion with a corresponding order of harmonics. Since the establishment of this technique in early 1980s, the discussion of its convergence has always been a hot topic, even up to now.[15–19] In 1993, Li and Haggans reported that the slow convergence was attributed to the use of slowly convergent Fourier expansion for the permittivity and the electromagnetic field in the grating region, through simulations of metallic gratings.[15] In 1996, Li revealed the reason why the inverse rule should be applied in case of complementary jump discontinuities, which helped achieve a faster convergence rate of RCWA under TM polarization.[16] Based on this explanation, Lalanne introduced a coefficient involving structural parameters for two-dimensional gratings, and managed to increase the convergence rate to some extent.[17] In 2007, Schuster et al. achieved a better convergence than the conventional formulations,[18] by combining the classic RCWA with Popov and Neviere's general equations.[19] For the purpose of a fast convergence rate, nearly all these contributions were striving to improve the modeling method itself.

Unlike these investigations, the convergence problem can be taken into account from another point of view. It is a universal approach to set up a high order of the Fourier harmonics in order to ensure the final convergence, in

most cases when applying the RCWA technique for optical modeling. However, the total number of floating point operations has a cubic relationship with the harmonic order.[20,21] This indicates that the technique will become rather time consuming if the expanded order is too high. Therefore, it is of great importance to choose an appropriate order to obtain high computational efficiency while maintaining sufficient accuracy. Supposing that a convergence order is able to be pre-established in terms of grating geometry and optical configuration, the consuming time will definitely be cut down to a large degree.

Concerning the correlation between the convergence order and model parameters, several general properties of the RCWA technique have been uncovered by a great number of simulations. Moharam et al. mentioned that the gratings with larger periods, deeper grooves, and under TM polarization or conical diffraction would require more harmonics to achieve the convergence results,[8] but this claim was not explained in detail. Bischoff also demonstrated that the classic RCWA showed serious drawbacks for the modeling of grating profiles with shallow slopes and multilayer stacks with many layers,[22] but again he did not explain in more detail. In fact, these researches provided a qualitative analysis of the convergence of the RCWA technique, rather than quantitative.

In this paper, we aim at discovering the quantitative relationship between the convergence order and the structural or optical parameters through numerical simulations, and providing guidance for the selection of an appropriate order when applying the RCWA technique. With a brief introduction of the RCWA theory in Sec. 2, we will present several simulations performed under different structural or optical conditions for binary rectangular groove gratings in Sec. 3. Finally in Sec. 4, the estimations of the convergence order will be made for some samples according to the observations.

2 Theory for the Rigorous Coupled-Wave Analysis

Without losing the generality of the optical modeling, a binary rectangular groove grating is selected in our simulation, and its geometry is depicted in Fig. 1. Any multilayer structures with arbitrary profiles can be investigated on this basis.[13] A linearly monochromatic light is launched into the sample at a polar angle θ derived away from the Z axis, and an azimuthal angle Φ between the plane of incidence and the grating vector along the direction normal to the walls. The angle ψ from the electric vector to the plane of incidence is called a polarized angle. Generally, this problem is named conical diffraction. When Φ approaches zero, which is called planar diffraction, the E-vector is normal ($\psi = 90$ deg) and parallel ($\psi = 0$ deg) to the plane of incidence for transverse electric (TE) and transverse magnetic (TM) polarization, respectively. The wavelength of the illuminated light in free space is λ_0. The refractive indices of superstrate and substrate are n_{I} and n_{II}, respectively. The periods Λ are made up of ridges and grooves, in which the refractive indices are n_{rd} and n_{gr}, respectively. The materials of the resist and substrate layers are Si_3N_4 and silicon, respectively. f is the fraction of the grating period occupied by the resist, with the depth d along the Z axis.

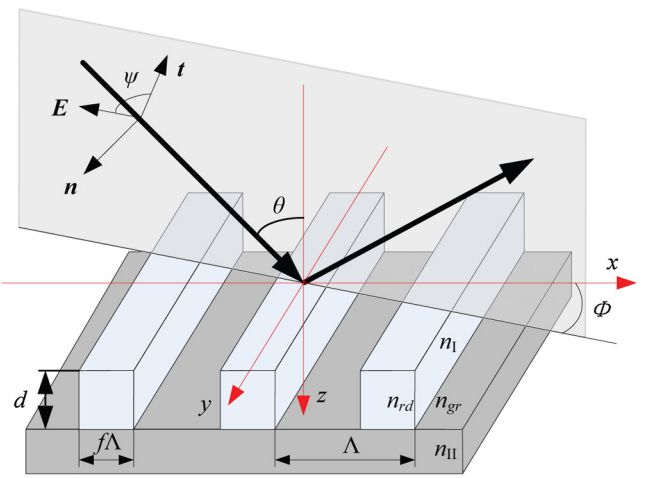

Fig. 1 Geometry of the binary rectangular groove grating.

For TE polarization, the incident normalized electric field can be expressed as

$$E_{\mathrm{inc},y} = \exp[-jk_0 n_1(\sin\theta x + \cos\theta z)], \tag{1}$$

where $k_0 = 2\pi/\lambda_0$. The Rayleigh expansions of the electric field of the reflected and transmitted region are

$$E_{\mathrm{I},y} = E_{\mathrm{inc},y} + \sum_i R_i \exp[-j(k_{xi}x - k_{\mathrm{I},zi}z)], \tag{2a}$$

$$E_{\mathrm{II},y} = \sum_i T_i \exp\{-j[k_{xi}x + k_{\mathrm{II},zi}(z-d)]\}, \tag{2b}$$

respectively, where k_{xi} can be determined from the Floquet condition and is given by

$$k_{xi} = k_0[n_1 \sin\theta - i(\lambda_0/\Lambda)], \tag{3}$$

and where $k_{m,zi}$ is calculated from the obtained k_0 and k_{xi}

$$k_{m,zi} = \begin{cases} +k_0[n_m^2 - (k_{xi}/k_0)^2]^{1/2} & k_0 n_m > k_{xi} \\ -jk_0[(k_{xi}/k_0)^2 - n_m^2]^{1/2} & k_{xi} > k_0 n_m \end{cases}, \quad m = \mathrm{I}, \mathrm{II}. \tag{4}$$

It is always necessary to have in mind the physical meaning that the ith wave is propagating when $k_0 n_m > k_{xi}$, and evanescent when $k_{xi} > k_0 n_m$. R_i and T_i are the normalized electric-field amplitudes of the ith reflected and transmitted wave, respectively.

The magnetic field in the reflected and transmitted region can be obtained from Maxwell's equations

$$\boldsymbol{H} = \left(\frac{j}{\omega\mu}\right)\nabla \times \boldsymbol{E}, \tag{5}$$

where μ is the permeability of the region and ω is the angular optical frequency.

In the grating region ($0 < z < d$), Eq. (5) can be simplified in a scalar form as

$$\frac{\partial E_y}{\partial z} = j\omega\mu_0 H_x, \tag{6a}$$

$$\frac{\partial H_x}{\partial z} = j\omega \in_0 \varepsilon(x) E_y + \frac{\partial H_z}{\partial x}, \tag{6b}$$

where $\in_0$ is the permittivity of free space, and ε is the permittivity of the grating region and can be expanded in a Fourier form. The electric field along the Y-axis and magnetic field along the X-axis may also be expressed with a Fourier expansion in terms of the space-harmonics field as

$$E_{gy} = \sum_i S_{yi}(z) \exp(-jk_{xi}x), \tag{7a}$$

$$H_{gx} = -j\left(\frac{\in_0}{\mu_0}\right)^{1/2} \sum_i U_{xi}(z) \exp(-jk_{xi}x), \tag{7b}$$

where $S_{yi}(z)$ and $U_{xi}(z)$ are the normalized amplitudes of the ith space-harmonic fields. Substituting Eq. (7) into Eq. (6), and eliminating H_z, we are able to obtain the coupled-wave equations as follows

$$\frac{\partial S_{yi}}{\partial z} = k_0 U_{xi}, \tag{8a}$$

$$\frac{\partial U_{xi}}{\partial z} = \left(\frac{{k_{xi}}^2}{k_0}\right) S_{yi} - k_0 \sum_p \varepsilon_{i-p} S_{i-p}, \tag{8b}$$

or, in a matrix form

$$\begin{bmatrix} \partial \mathbf{S}_y / \partial(z') \\ \partial \mathbf{U}_x / \partial(z') \end{bmatrix} = \begin{bmatrix} \mathbf{0} & \mathbf{I} \\ \mathbf{A} & \mathbf{0} \end{bmatrix} \begin{bmatrix} \mathbf{S}_y \\ \mathbf{U}_x \end{bmatrix}, \tag{9}$$

where $z' = k_0 z$, and $\mathbf{A} = \mathbf{K}_x^2 - \mathbf{E}$. By eliminating $\mathbf{U}_x$, Eq. (9) can be reduced to

$$[\partial^2 \mathbf{S}_y / \partial(z')^2] = [\mathbf{A}][\mathbf{E}], \tag{10}$$

then the eigenvalue decomposition is able to be carried out more efficiently. By diagonalizing $\mathbf{A}$, the solution can be written as follows

$$S_{yi}(z) = \sum_m w_{i,m} \{ {c_m}^+ \exp(-k_0 q_m z) + {c_m}^- \exp[k_0 q_m (z-d)] \}, \tag{11a}$$

$$U_{xi}(z) = \sum_m v_{i,m} \{ -{c_m}^+ \exp(-k_0 q_m z) + {c_m}^- \exp[k_0 q_m (z-d)] \}, \tag{11b}$$

where $w_{i,m}$ is the (i, m)'th element of the eigenvector matrix $\mathbf{W}$, q_m is the m'th element of the positive square root eigenvalue matrix $\mathbf{Q}$, regarding $\mathbf{A}$, and $v_{i,m}$ is the (i, m)'th element of the eigenvector matrix $\mathbf{V}$, which can be obtained from $\mathbf{V} = \mathbf{WQ}$.

By setting up boundary value conditions of the tangential electric and magnetic field components, the coupled-wave equations can be solved. With the normalized electric-field amplitudes of the reflected wave, reflectivity in each diffraction order can be calculated.

Formulations of RCWA under TM polarization and conical diffraction could be derived in a similar way. Note that during the expansion of permittivity in the coupled-wave equations, the inverse rule should be applied in place of Laurent's rule to achieve a faster convergent result, according to Li's point of view.[16] Those formulation details are omitted here.

3 Simulation and Analysis

Before introducing the simulation results, it is important to point out that all the structural and optical parameters will affect the convergence to a greater or less degree. We attempted to achieve repeatability and validity of the properties handled here, however, conceivable simulations could hardly be exhausted since the combinations of the parameters are extremely numerous. Multiple simulations have been carried out using different optical and structural parameters, especially the ones in common use, with only a small number of them listed here. Given the generality of the characteristics we observe, both the planar diffraction (TE and TM polarization) and conical diffraction have been taken into account. Consequently, it is considered that the characteristics listed below may be applicable in many cases, at least in a specific range.

3.1 *Simulation Under Varied Grating Period*

By varying the period Λ while fixing other structural parameters (including f and d) and optical parameters (including λ, θ, Φ and ψ), we are able to obtain some meaningful results as shown in Fig. 2. The convergence order is labeled as an integer N on the vertical axes. The graph shows that the convergence orders have an approximately linear correlation with the periods. They are fit by linear functions and clearly demonstrated that the convergence orders calculated under different periods are distributed around the linear regression lines.

Considering the general linearity found above, we performed other simulations under conical diffraction with different structural and optical parameters, such as f, d, and θ, with results shown in Fig. 3(a), 3(b), and 3(c), respectively. It is apparent that the convergence orders keep a linear growth along the horizontal axes on varied f, θ, and d, except that the deviation under the depth of 2 μm is much more remarkable than the other data.

We also performed quantitative analysis for varied f, d, and θ, with the linear correlation coefficients under three polarization states shown in Fig. 4(a), 4(b), and 4(c), respectively. The vertical axis R stands for the correlation coefficient calculated with given structural and optical parameters, within the range between 0 and 1. It is observed from Fig. 4(a) that the correlation coefficients range from 0.9 to 1, corresponding to the small deviations in Fig. 3(a). A downward trend is noticed from Fig. 4(b) along the horizontal axis for all the three polarization states, which means that the linear correlations are no longer typical for deep grooves, as can be seen in Fig. 3(b). The correlation coefficients for varied θ are still satisfactory with the range between 0.8 and 1, even though the deviations along the regression lines shown in Fig. 3(c) are much larger than those in Fig. 3(a). In addition, the linear correlations don't differ significantly among the three polarization states, with the correlation coefficients under TM polarization slightly

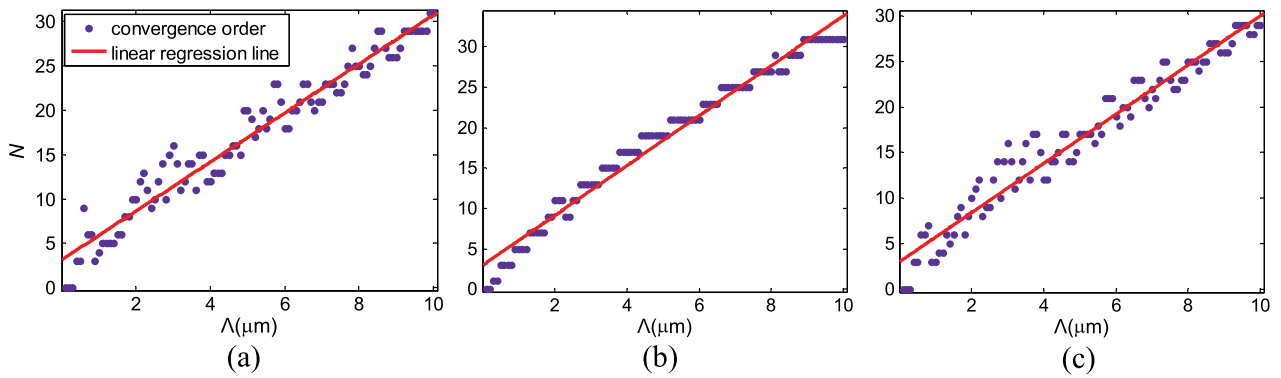

Fig. 2 The convergence orders calculated in varied period Λ, while other parameters are fixed in $f = 0.5$, $d = 0.2$ μm, $\lambda = 0.5$ μm. (a) transverse electric (TE) polarization ($\theta = 10$ deg), (b) transverse magnetic (TM) polarization ($\theta = 10$ deg), and (c) conical diffraction ($\theta = 10$ deg, $\varphi = 30$ deg, $\psi = 45$ deg). The reflectivities calculated with the truncation order of 200 are considered as references, and convergence orders are picked up on an error bound of 0.2%. This indicates that the error corresponding to the reference is no more than 0.2% if any order higher than the convergence order is selected.

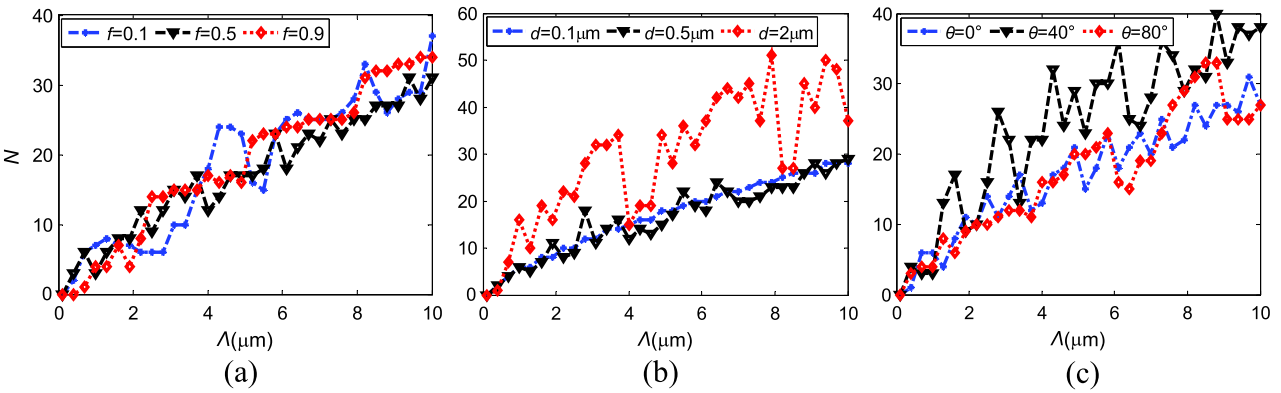

Fig. 3 Convergence orders under conical diffraction for (a) varied duty cycle f, (b) varied depth d, and (c) varied incidence angle θ.

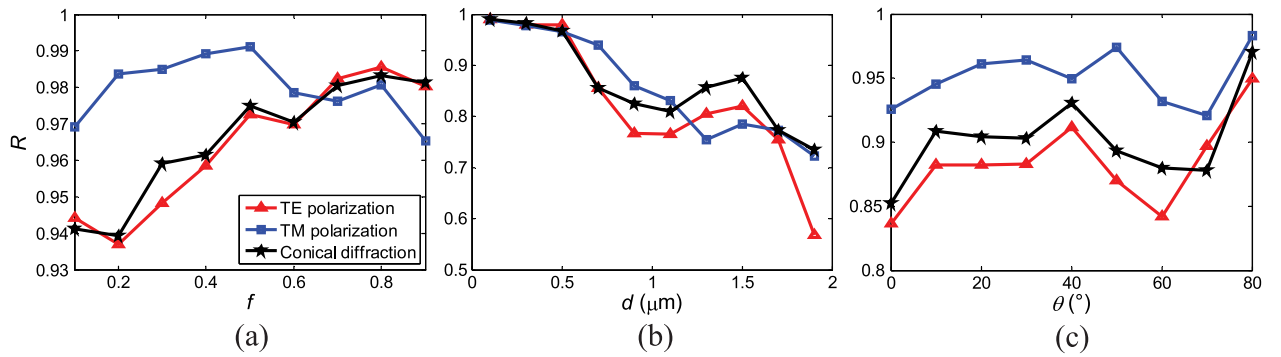

Fig. 4 Correlation coefficients for (a) varied duty cycle f, (b) varied depth d, and (c) varied incidence angle θ under three polarization states [transverse electric (TE) polarization, transverse magnetic (TM) polarization, and conical diffraction].

higher than the other two states in general. On the whole, the results indicate that the linearity exists in a variety of structures and optical configurations, rather than merely limit to a specific system.

3.2 *Simulation Under Varied Illuminated Wavelength*

In OCD metrology, such as reflectometry and scatterometry, illuminated wavelength can be adjusted in most cases. Therefore, simulations have been carried out by setting up different illuminated wavelengths, with the results shown in Fig. 5. The dash lines are for simulation data and the solid lines for regression. It is noted that the linearity is again nearly independent of the wavelength, and that the illuminated wavelength is intimately related to on the convergence order, when we fix all the structural parameters. With a fixed structure, the convergence order decreases with the growth of wavelength. It is also observed that the slopes of the linear regression lines are dependent on the wavelengths to a great extent, while the intercepts have little correlation with them.

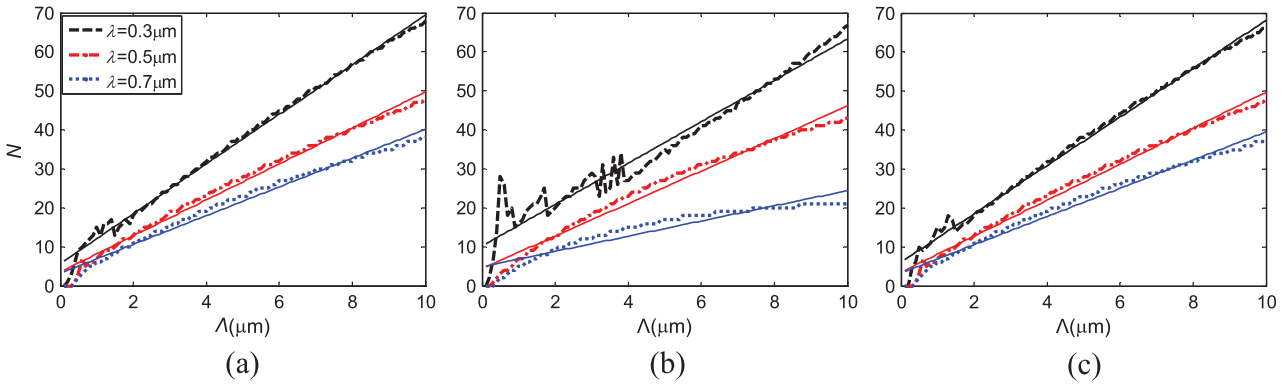

Fig. 5 The convergence order calculated for three different wavelengths under (a) TE polarization, (b) transverse magnetic (TM) polarization, and (c) conical diffraction. Other parameters are the same as those listed in Fig. 2. The dash and solid lines represent the simulated and the linear regression results respectively.

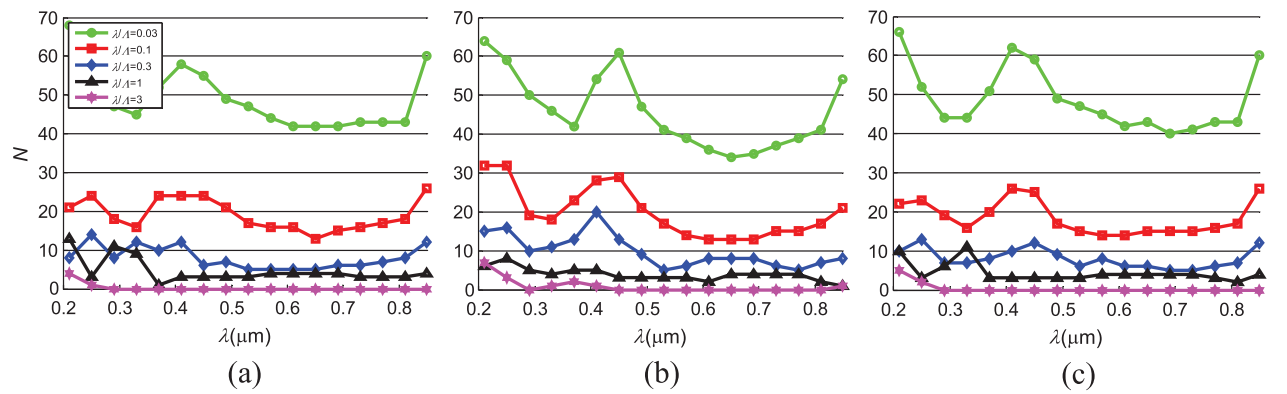

Fig. 6 Simulations under different ratios of λ to Λ under (a) transverse electric (TE) polarization, (b) transverse magnetic (TM) polarization, and (c) conical diffraction. Other parameters are the same as those listed in Fig. 2. It should be noticed that the grating period is modulation by the fixed ratio, even though the horizontal axis is depicted as the illuminated wavelength.

3.3 *Simulation Under Varied Ratio of Illuminated Wavelength to Grating Period*

We carried out further study and focused on the approximately invariance of the intercepts of different regression lines. The ratio of the illuminated wavelength to the grating period is fixed in the following simulation. The ratio is set to 0.03, 0.1, 0.3, 1, and 3 sequentially, with results depicted in different colors in Fig. 6. It is interesting to note that the lower the ratio is, the more order it needs to achieve convergence. When the ratio is set at 3, even the permittivity and electric and magnetic field expanded into 0th order can achieve a satisfactory result. The convergence order in each ratio has occupied a limited order range compared to the whole vertical axis. In different ranges of illuminated wavelengths, it can be seen that in the range of 0.5 to 0.8 μm, approximately the visible band, the jump of the convergence order under each ratio varies more slightly than that in the ultraviolet band, which can be observed in TE, TM polarization and conical diffraction. It is thus possible to estimate the order with given structural and optical parameters.

4 Application in Some Estimations of the Convergence Order

From the results shown in Sec. 3, especially those phenomena observed in Fig. 6, we can estimate the convergence order with given structural and optical parameters. Since the jump in the visible range is slighter than in other ranges, we are more likely to estimate an accurately convergent result for a specific structure. The structural and optical parameters for estimations are listed in Table 1. The value f is 0.5 in our simulation, and d is fixed at 0.2 μm. Assuming that it follows the normal distribution, the 95% confidence interval

Table 1 Simulation parameters for estimations.

Serial number	λ (μm)	Λ (μm)	Ratio of λ to Λ	Polarization state
1	0.5	16.7	0.03	TE polarization
2	0.6	6	0.1	TM polarization
3	0.7	2.33	0.3	TE polarization
4	0.8	0.8	1	TM polarization
5	0.5	16.7	0.03	Conical diffraction
6	0.6	6	0.1	Conical diffraction
7	0.7	2.33	0.3	Conical diffraction
8	0.8	0.8	1	Conical diffraction

Table 2 Results of estimations.

Serial number	μ	σ	Confidence interval	Selected order	Error (%)
1	43.7	2.0	[42.9, 44.4]	45	0.33
2	14.5	1.8	[13.9, 15.2]	16	0.01
3	5.9	0.9	[5.5, 6.2]	7	0.18
4	3.3	0.8	[3.0, 3.6]	4	0.17
5	43.1	2.3	[42.2, 44.0]	45	0.07
6	15.1	1.0	[14.7, 15.5]	16	0.09
7	6.3	1.2	[5.9, 6.8]	7	0.07
8	3.7	0.5	[3.5, 3.9]	4	0.14

is calculated through the data in the wavelength range of 0.5 to 0.8 μm. With this confidence interval, an order above the interval has been selected to calculate the reflectivity.

Table 2 shows the results of the estimations. It is noted that the selected order is much less than the reference order (200), especially when the ratio is high. Meanwhile, most of the achieved accuracy is satisfactory, except the first sample exceeds the expected error bound of 0.2%. These results thus demonstrate that the estimations carried out here are effective in most cases.

5 Conclusions

In this paper, several sets of simulations have been carried out to find out some relationship between the convergence order and the structural or optical parameters for binary rectangular groove gratings. It is observed that the structural dimension and the illuminated wavelength have a combined effect on the convergence order, and the ratio between them could weaken this effect. It is also noticed that in a certain range of wavelength, the jump of convergence order is relatively slight. These observations may provide some guidelines for the estimation of convergence order for a specific sample, and most of the estimations have shown satisfactory accuracy compared to the reference.

Acknowledgments

This work was funded by National Natural Science Foundation of China (Grant Nos. 91023032 and 51005091), National Instrument Development Specific Project of China (Grant No. 2011YQ160002), and Postdoctoral Science Foundation of China (Grant No. 20100470052).

References

1. R. K. Leach et al., "The European nanometrology landscape," *Nanotechnology* **22**(6), 062001 (2011).
2. X. Niu et al., "Specular spectroscopic scatterometry," *IEEE Trans. Semicond. Manuf.* **14**(2), 97–111 (2001).
3. C. Raymond, "Overview of scatterometry applications in high volume silicon manufacturing," *AIP Conf. Proc.* **788**, 394–402 (2005).
4. M. Foldyna et al., "Critical dimension of biperiodic gratings determined by spectral ellipsometry and Mueller matrix polarimetry," *Eur. Phys. J. Appl. Phys.* **42**(3), 351–359 (2008).
5. C. G. Frase, E. Buhr, and K. Dirscherl, "CD characterization of nanostructures in SEM metrology," *Meas. Sci. Technol.* **18**(2), 510–519 (2007).
6. N. G. Orji and R. G. Dixson, "Higher order tip effects in traceable CD-AFM-based linewidth measurements," *Meas. Sci. Technol.* **18**(2), 448–455 (2007).
7. Y. Nakata and M. Koshiba, "Boundary-element analysis of plane-wave diffraction from groove-type dielectric and metallic gratings," *J. Opt. Soc. Am. A* **7**(8), 1494–1502 (1990).
8. M. G. Moharam, E. B. Grann, and D. A. Pommet, "Formulation for stable and efficient implementation of the rigorous coupled-wave analysis of binary gratings," *J. Opt. Soc. Am. A* **12**(5), 1068–1076 (1995).
9. H. Ichikawa, "Electromagnetic analysis of diffraction gratings by the finite-difference time-domain method," *J. Opt. Soc. Am. A* **15**(1), 152–157 (1998).
10. T. Grosges, A. Vial, and D. Barchieshi, "Models of near-field spectroscopic studies: comparison between finite-element and finite-difference methods," *Opt. Express* **13**(21), 8483–8497 (2005).
11. M. Foldyna et al., "Reconstruction of grating parameters from ellipsometric data," *Proc. SPIE* **5445**, 226–229 (2004).
12. H. Gross et al., "Computational methods estimating certainties for profile reconstruction in scatterometry," *Proc. SPIE* **6995**, 69950T (2008).
13. M. G. Moharam, D. A. Pommet, and E. B. Grann, "Stable implementation of the rigorous coupled-wave analysis for surface-relief gratings: enhanced transmittance matrix approach," *J. Opt. Soc. Am. A* **12**(5), 1077–1086 (1995).
14. W. Lee and F. L. Degertekin, "Rigorous coupled-wave analysis of multilayered grating structures," *J. Lightwave Tech.* **22**(10), 2359–2363 (2004).
15. L. Li and C. W. Haggans, "Convergence of the coupled-wave method for metallic lamellar diffraction gratings," *J. Opt. Soc. Am. A* **10**(6), 1184–1189 (1993).
16. L. Li, "Use of Fourier series in the analysis of discontinuous periodic structures," *J. Opt. Soc. Am. A* **13**(9), 1870–1876 (1996).
17. P. Lalanne, "Improved formulation of the coupled-wave method for two-dimensional gratings," *J. Opt. Soc. Am. A* **14**(7), 1592–1598 (1997).
18. T. Schuster et al., "Normal vector method for convergence improvement using the RCWA for crossed gratings," *J. Opt. Soc. Am. A* **24**(9), 2880–2890 (2007).
19. E. Popov and M. Neviere, "Maxwell equations in Fourier space: fast-converging formulation for diffraction by arbitrary shaped, periodic, anisotropic media," *J. Opt. Soc. Am. A* **18**(11), 2886–2894 (2001).
20. H. Chu, "Finite difference approach to optical scattering of gratings," *Proc. SPIE* **5188**, 358–370 (2003).
21. P. L. Jiang et al., "Forward solve algorithms for optical critical dimension metrology," *Proc. SPIE* **6922**, 69221O (2008).
22. J. Bischoff, "Improved diffraction computation with a hybrid C-RCWA-Method," *Proc. SPIE* **7272**, 72723Y (2009).

Shiyuan Liu is a professor of mechanical engineering at Huazhong University of Science and Technology, leading his nanoscale and optical metrology group with research interest in the metrology and instrumentation for nanomanufacturing. He also actively works in the area of optical lithography, including partially coherent imaging theory, wavefront aberration metrology, optical proximity correction, source mask optimization, and inverse lithography technology. He received his PhD in mechanical engineering from Huazhong University of Science and Technology in 1998. He is a member of SPIE, OSA, AVS, IEEE and CSMNT (Chinese Society of Micro/Nano Technology). He holds 12 patents and has authored or co-authored more than 100 technical papers.

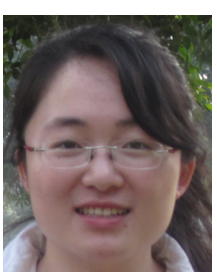

Yuan Ma is a graduate student at Huazhong University of Science and Technology, pursuing her MS degree in mechanical engineering under the guidance of Prof. Shiyuan Liu. She received her BS degree in mechanical engineering from Nanjing University of Science and Technology in 2009. Her research interests include nanometrology and optical modeling based on computational electromagnetic methods.

Xiuguo Chen is currently a PhD candidate at Huazhong University of Science and Technology under the guidance of Prof. Shiyuan Liu. He received his MS degree from the School of Mechanical Science and Engineering of the same university in 2009. His research involves various issues in optical critical dimension (OCD) metrology, including fast optical modeling and robust parameter extraction. He is a student member of OSA and ACM.

Chuanwei Zhang is a postdoctoral research associate at Huazhong University of Science and Technology. He received his BS and MS in mechanical engineering from Wuhan University in 2004 and 2006, respectively, and then received his PhD in mechanical engineering from Huazhong University of Science and Technology in 2009. He is currently working on optical techniques for critical dimension, overlay, and 3D profile metrology for nanomanufacturing.